Electrochimica Acta 286 (2018) 179–186

Contents lists available at ScienceDirect

Electrochimica Acta

journal homepage: www.elsevier.com/locate/electacta

A cross examination of electron transfer rate constants for carbon screen-printed electrodes using Electrochemical Impedance Spectroscopy and cyclic voltammetry

Edward P. Randviir

Faculty of Science and Engineering, School of Chemistry and the Environment, Division of Chemistry and Environmental Science, Manchester Metropolitan University, Chester Street, Manchester M1 5GD, Lancs, UK

ARTICLE INFO

Article history:
Received 24 May 2018
Received in revised form
2 August 2018
Accepted 6 August 2018
Available online 9 August 2018

Keywords:
Electrochemistry
Cyclic voltammetry
Electrochemical impedance spectroscopy
Rate constant
Nicholson

ABSTRACT

Heterogeneous electron transfer rate constants of a series of chemical systems are estimated using Cyclic Voltammetry (CV) and Electrochemical Impedance Spectroscopy (EIS), and critically compared to one another. Using aqueous, quasi-reversible redox systems, and carbon screen-printed electrodes, this work has been able to quantify rate constants using both techniques and have proved that the two methods sometimes result in measured rate constants that differ by as much as one order of magnitude. The method has been converted to estimate k^0 values for irreversible electrochemical systems such as ascorbic acid and norepinephrine, yielding reasonable values for the electron transfer of their respective oxidation reactions. Such electrochemically irreversible cases are compared to data obtained *via* digital simulations. The work is limited to finite concentration ranges of electroactive species undergoing simple electron processes ('E' type reactions). The manuscript provides the field with a simple and effective way estimating electron transfer rate constants for irreversible electrochemical systems without using digital software packages, something which is not possible using either Nicholson or Laviron methods.

1. Introduction

In electrochemistry, the estimation of the heterogeneous electron transfer rate constant, k^0, is of paramount interest when the performance of electrode materials are examined. The rate constant gives the user an indication of the speed of electron transfer between an electroactive species and an electrode surface, whether the electrode material determines the overall rate of the electrochemical reaction, and could even be used to estimate the allotrope of the material in question [1]. As it stands, k^0 is one of the strongest pieces of information one can extract through use of electrochemical techniques; hence users have been reporting k^0 values voltammetrically since at least 1956/1957 when the theory of electron transfer was reported by Marcus [2–4], and impedimetrically since at least 1947 when Randles studied the kinetics of mercury electrodes [5].

Over time, there has been little diversity in terms of experimental determination of the k^0 of a given system. The most popular method for the determination of k^0 is Cyclic Voltammetry (CV), since Marcus theory was first reported. Electrochemists commonly take ideas developed by Nicholson [6–8] to estimate the k^0 values for their electrode material. A typical procedure is to investigate the peak-to-peak separation, ΔE_P (see Fig. 1), of a redox couple as a function of scan rate in a quasi-reversible system. The Nicholson method introduces the dimensionless parameter, ψ, which is plotted against the ΔE_P for a given system to produce a working curve. The dimensionless parameter thus indicates electrochemical reversibility (where $\psi = 20$, the system is reversible; where $\psi \leq 7$, the system is quasi-reversible) and is fitted to ΔE_P to analyse electrochemical systems, such as cadmium reduction which was reported originally [8]. Today, this process is made much simpler by the excellent work reported by Lavagnini et al. [9] Their work takes Equation (1), which is the link between the dimensionless parameter ψ and k^0, and reports it graphically by calculating ψ from the ΔE_P, X, in mV (Equation (2)):

$$\psi = k^0[\pi DnF\upsilon/RT]^{-\frac{1}{2}} \quad (1)$$

$$\psi = (-0.6288 + 0.0021X)/(1 - 0.017X) \quad (2)$$

E-mail address: E.Randviir@mmu.ac.uk.

https://doi.org/10.1016/j.electacta.2018.08.021

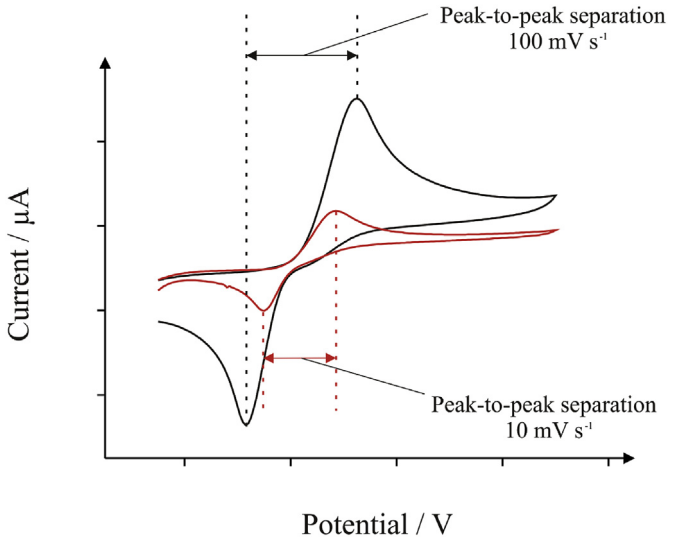

Fig. 1. Cyclic voltammetry profiles typical of 0.5 mM hydroquinone in pH 7.4 phosphate buffer solution, illustrating the increase in ΔE_P as the scan rate increases.

where D is the diffusion coefficient of the electroactive species, n is the number of electrons transferred in the electrochemical reaction, F is the Faraday constant, R is the molar gas constant, and T is the absolute temperature. Through this mathematical manipulation, k^0 is taken directly from the slope of the graph of ψ *versus* $[\pi DnF\nu/RT]^{-1/2}$. The method improves the Nicholson method by not only making quantitative evaluation of the rate constant easier, but also by extending the working range of the Nicholson parameter towards significantly higher (and lower) peak potentials. These principles have been applied to estimate electron transfer rates of many materials; Table 1 disseminates some electrode materials and lists their reported heterogeneous electron transfer rate constants. There is an obvious limitation of this method, however. The method only works for quasi-reversible systems, because it relies upon the fact that a quasi-reversible system will increase its ΔE_P as the scan rate increases, because the rate of mass transport is becoming quicker than or equal to the rate of electron transfer in this case. Furthermore, systems with high solution resistance or capacitance give rise to errors in the CV-determination of electron transfer rate constants using the Nicholson method because current signals are masked by non-Faradaic effects. Another limitation of this approach is that the method is limited when the ΔE_P values increase beyond 212 mV, which precludes examination of electron transfer rate constants for irreversible systems too. Despite the limitations to the Nicholson method, it is still used by electrochemists today, but often in a revised format such as in Lavagnini's work (*vide supra*) [9].

k^0 values can be measured using digital simulations for both electrochemically reversible and irreversible cases, while

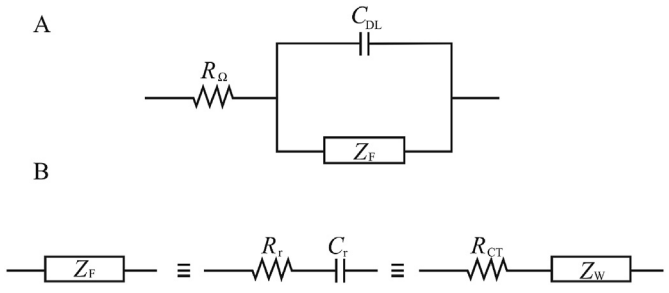

Scheme 1. A: Randles model of an equivalent circuit incorporating solution resistance (R_Ω), double layer capacitance (C_{DL}), and series impedance (Z_F). B: The series impedance component and equivalent models incorporating series resistance (R_r) and pseudocapacitance (C_r), and charge transfer resistance (R_{CT}) and Warburg impedance (Z_W).

Electrochemical Impedance Spectroscopy (EIS) is another method which has the ability to measure k^0 values for charge transfer reactions and is thus useful for reversible reactions where CV is not suitable. The earliest example of the latter, to my knowledge, was by Randles, whose paper investigates the kinetics of rapid electrode reactions [5]. The paper introduces itself by stating that rapid electrode reactions are almost always described as being controlled by diffusion, because the rate of electron transfer cannot be limiting the overall reaction rate. However, one should not forget that the electron transfer still contributes to the rate, and hence the derived expression to quantify the electron transfer rates of 'reversible' electrode reactions. The impedance work on cadmium and thallium was the first of its kind in terms of proving that k^0 can be deduced from EIS by utilising Equation (3), where R_r is termed as the *series resistance* due to a Faradaic process, ω is the angular frequency and C_r is the *pseudocapacitance* due to the Faradaic process. Note in some old texts, R_r is also denoted as R_s, which is sometimes referred to as the polarization resistance. Some texts recommend against this terminology [10].

$$R_r - \frac{1}{\omega C_r} = \frac{RT}{n^2F^2AC}\cdot\frac{1}{k^0} \tag{3}$$

Practical utility of this equation has been limited, since researchers tend to use the Nicholson equation to determine electron transfer rate constants for electrode reactions. Furthermore, modern notation rarely sees terms such as R_r and C_r, and interpretation of how these components translate to modern notation (i.e. R_{CT} and Z_W) is rarely discussed. Scheme 1 depicts a Randles circuit for an electrochemical cell, split into its three contributory components: the solution resistance (R_Ω), in series with the double layer capacitance (C_{DL}) and the frequency-dependent impedance (Z_F). The frequency-dependent impedance component in the original work by Randles was modelled as an ideal resistor in series (R_r) with a pseudocapacitance (C_r) element, the summation of which became Z_F. In modern terminology, the resistance observed in the series impedance component is termed the charge transfer resistance

Table 1
A list of literature examples of electrode materials and their reported electron transfer rate constants, calculated *via* the Nicholson method. All values are determined *via* CV.

Electrode	Electroactive Species	k^0/cm s^{-1}	Ref.
Glassy carbon	Ferrocene[a]	1.45×10^{-4}	[26]
Micro-fabricated iridium	Potassium ferricyanide	7.39×10^{-2}	[27]
Glassy carbon	Superoxide	9.30×10^{-2}	[28]
Flexible graphite electrode	Hexaamine-ruthenium(III) chloride	1.72×10^{-3}	[29]
Monolayer CVD graphene	N, N, N′, N′-tetramethyl-p-phenylenediamine	1.81×10^{-3}	[30]
Platinum disk	Viologen	1.58×10^{-3}[b]	[31]

[a] The paper reports a multitude of analytes.
[b] In DMSO.

(R_{CT}), in series with impedance due to diffusion (Z_W). However, R_{CT} and R_r are not analogous; in fact, R_r is the summation of R_{CT} and diffusional components, taking into account the relative electron transfer coefficients (β) and diffusion regimes of both the oxidation and reduction processes of a redox couple, given by:

$$R_r = R_{CT} + \frac{\sigma}{\omega^{\frac{1}{2}}} \tag{4}$$

where:

$$\sigma = \frac{1}{nFA\sqrt{2}}\left(\frac{\beta_O}{D_O^{\frac{1}{2}}} - \frac{\beta_R}{D_R^{\frac{1}{2}}}\right) \tag{5}$$

Note ω is the frequency of the applied perturbation. Now it is seen from Equations (4) and (5) that R_{CT} is not directly translatable to R_r, since the R_{CT} model is for electron transfer only, and not diffusional impedance as a result of the development of concentration gradients at the electrode surface. For this reason, R_{CT} is only a valid measurement when $C_{OX} = C_{RED}$, and the experiment is measured at a high enough frequency such that Warburg impedance is not a factor in the impedance profile. Equation (4) is derived from Equation (6):

$$R_{CT} = R_r - \frac{1}{\omega C_r} \tag{6}$$

where:

$$C_r = \frac{1}{\sigma\omega^{\frac{1}{2}}} \tag{7}$$

R_{CT} reflects the charge transfer kinetics of an electrochemical reaction and is the ratio of the applied ac perturbation to the observed Faradaic (ac) current produced in an electrochemical reaction. The foundation of modern day impedimetric notation probably started with the series entitled "On the Impedance of Galvanic Cells" authored by J. H. Sluyters. In the first paper, Sluyters discussed the theory of galvanic cell impedance and hypothesized that parameters such as R_S, R_{CT}, and Z_W could be deduced from the real and imaginary parts of the total impedance data. Sluyters and Oomen then successfully determined k^0 for $Zn(Hg)/Zn^{2+}$ in a mixture of $NaClO_4$ and $HClO_4$, while simplifying the derivation of k^0 [11]. The authors reported that the charge transfer resistance, R_{CT} (denoted as θ in their work), calculated from equivalent circuit fitting in EIS experiments is inversely proportional to the exchange current density, i_0, *via* Equation (8) [12,13]:

$$R_{CT} = \frac{RT}{nFi_0}. \tag{8}$$

Also, i_0 is related to k^0 *via* equation (9) [12,13]:

$$i_0 = nFAk^0C, \tag{9}$$

so it follows that [13]:

$$R_{CT} = \frac{RT}{n^2F^2ACk^0}. \tag{10}$$

These equations assume equimolar concentrations of oxidised and reduced species at the electrode surface at a given point in time, which becomes very important for EIS determination of k^0. The original report by Randles states that the derivation of Equation (3), and consequently Equation (10), is for the case when the electrode process is so rapid that it can be termed reversible. Whilst this needs to be kept in mind throughout, the inference is that the equation can also be applied to other simple electrochemical systems because EIS takes into account diffusional processes through manipulation of the real and imaginary components of EIS spectra. Equation (10) has proven to be practical in a number of cases – as highlighted by the work presented in Table 2.

The focus of this paper is to critically compare k^0 values for a range of systems using CV and EIS. This work also provides a graphical method to measure k^0 using EIS, as was the case in the work by Lavagnini with the Nicholson method [9]. This work could provide a very useful method for the case of electrochemically irreversible systems where k^0 cannot be measured utilising the Nicholson method, as the data analysis for this method takes place at one charge transfer reaction instead of observing the differences between two, which cannot be done in the case of an electrochemically irreversible system.

2. Experimental

2.1. Chemicals

All chemicals were of the highest grade commercially available and obtained from Sigma-Aldrich (UK). All solutions were prepared using deionised water of resistivity of no less than 18.2 MΩ cm. All electroactive materials were dissolved in pH 7.4 Phosphate Buffer Solution (PBS) with 0.1 M KCl as a supporting electrolyte. Hydroquinone, ascorbic acid, and dopamine solutions were prepared on the day of testing and kept in the dark. Potassium hexachloroiridate was used as a reference redox probe.

2.2. Apparatus

Electrochemical measurements were performed at ambient temperature (22 ± 2 °C) using an Ivium CompactStat™ (Netherlands), housed in a grounded home-built copper mesh Faraday cage. The software package was IviumSoft. The selected cell configuration comprised of a screen-printed three electrode system including a carbon working and auxiliary electrode, and an Ag/AgCl reference electrode. The electrodes were printed in-house as reported previously [14–16]. Briefly, a layer of appropriate carbon ink is printed onto a polyester substrate and cured at 60 °C for 30 min. Second, a Ag/AgCl paste is printed on top of the reference area of the electrode and cured at 60 °C for a further 30 min. Finally, a dielectric is printed on top to protect the electrode connections and define the working, auxiliary, and reference sections of the electrode. The electrodes are cured once more at 60 °C for 30 min. The electrodes are then ready for experimentation. The same procedure is applied to all the different electrodes utilised in this work: Edge plane-like SPE ink (ESPE); Low Resistance Ink SPE (LRI-SPE); Basal plane-like SPE (BSPE); and Graphene SPE (GSPE).

2.3. Electrochemical parameters

The electrochemical cell was 25 mL in volume and composed of

Table 2
A list of electrode materials and their reported electron transfer rate constants, determined *via* EIS and modelled using Equation (6).

Electrode	Electroactive Species	k^0/cm s^{-1}	Ref.
Gold	Potassium ferricyanide	0.48	[32]
Pt/PEDOT	Potassium ferricyanide	8.80×10^{-3}[a]	[33]
Glassy carbon	Potassium ferricyanide	1.30×10^{-3}	[34]
Glassy carbon	Guanine	6.21×10^{-3}	[35]
Glassy carbon	Dopamine	5.40×10^{-4}	[36]

[a] Rate constant quoted for 63.7 mC cm^{-2} polymerisation charge with 1 mM potassium ferricyanide.

the target material dissolved within 0.1 M pH 7.4 phosphate buffer solution and 0.1 M KCl, unless otherwise stated. Voltammetric potential windows differ depending upon the electroactive species and will be discussed separately in each section. The EIS excitation potential in each case is equal to the half wave potential of the oxidation process using cyclic voltammetry at 100 mV s^{-1}. This is to ensure equimolar concentrations of the oxidised and reduced species at the electrode surface at all times. Voltammetric measurements were performed with a +10 mV potential step. A new electrode was used between measurements. The frequency range selected for EIS was 10000–0.2 Hz. The EIS spectra were modelled using a simple Randles circuit (Fig. 2B) in Ivium Equivalent Circuit Evaluator. The amplitude of the ac voltage applied in EIS experiments was 10 mV.

2.4. Electrode compositions and characteristics

The electrodes utilised in this work are defined above. The inks for the different SPEs were all obtained commercially and are detailed as follows: ESPE (Product Code: C2000802P2; Gwent Electronic Materials Ltd, UK); BSPE – (Product Code: ED5020; Electra Polymers Ltd, UK); GSPE (Product Code: HDPlas™ Graphene Ink SC213; Haydale Ltd, UK); and LRI-SPE (Product Code: C2130925D1; Gwent Electronic Materials Ltd, UK). ESPE has been characterised previously [14] and exhibits 39.0–41.0% solid content, suspended in diacetone alcohol (solvent makes up 35% of the ink) according to the manufacturer. ESPE also exhibits a viscosity of 2.0–3.5 Pa and an ink screen life of three hours. The composition deficit is made up of carbon black to improve the conductivity of the ink, providing the ink with its edge plane-like properties. The BSPE ink is described as a thermal carbon conductor paste. The specific details of the ink are withheld by the manufacturer, but their Materials Safety Datasheet (MSDS) alludes to the carbon being suspended in a mixture of solvents, namely 2-(2-butoxyethoxy)ethanol (30–60%), formaldehyde (<0.1%), isopropyl alcohol (0.1–1%), n-butanol (0.1–1%), and phenol (<0.1%). The basal-like characteristics are assumed to be typical of the presence of polymeric binders, as discussed by Choudry et al. [15] The GSPE ink has been characterised previously [14] where it was revealed that it is a carbon-based carrier ink (43–45% solid content) with a viscosity of 8.0–11.0 Pa and an ink screen life of three hours. The ink is loaded with small amount of carbon black, to improve conductivity, and contains graphene nanoplatelets produced *via* a split plasma process, resulting in graphene which is lacking in structural damage. The LRI-SPE contains 39.0–41.5% solid content and exhibits a viscosity of 8.0–11.0 Pa, with an ink screen life of over three hours. The ink is designed to exhibit a high conductance (hence, low resistivity) and thus should be ideal for impedance measurements.

2.5. Limitations of screen-printed electrodes

The author acknowledges some inherent limitations with SPEs throughout the work. Indeed, more conventional electrodes (e.g. gold, glassy carbon) could have been chosen for these experiments. At the time of data collection, such conventional electrodes were unavailable to the author and hence the data was exclusively collected using SPEs. The major limitation of SPEs in the context of this work is the non-uniform topography (i.e. unpolished) causing heterogeneous electron transfer at different rates across the surface. However, it should also be noted that previous works have identified the rate constant on a macro-scale to differ with a %RSD under 5% (see Randviir et al. [14]), and therefore the author believes the electrodes to be analytically useful under the conditions outlined within this manuscript. Another limitation of such electrodes is the intentional inclusion of binders to "slow" the electron transfer rate kinetics in the case of the BSPE. It should be stated that the binders are inserted in a known capacity, resulting in a high level of kinetic control. SEM images of the electrode surfaces are provided in Reference [15] for interested readers. Further, the surface roughness of the SPEs is a potential factor influencing the EIS response. Indeed, previous reports focussing on the change in electron transfer rate constant using polished *versus* unpolished SPEs indicated that polishing the surface is beneficial for inner-sphere redox probes, while the effect upon outer-sphere redox probed was unaffected [17]. The authors in this case ascribe the changes in voltammetric behaviour to the change in carbon/oxygen ratio at the electrode surface, which is widely known to influence change transfer.

3. Results and discussion

To robustly test k^0 values, the voltammetric k^0 values of dopamine and hydroquinone utilising the modified Nicholson method is first explored [9]. This is easily tested by investigating the ΔE_P as a function of scan rate, according to Equations (1) and (2). The voltammetric responses of dopamine and hydroquinone are presented in Fig. 3A and B, respectively. In both cases, the peak current is

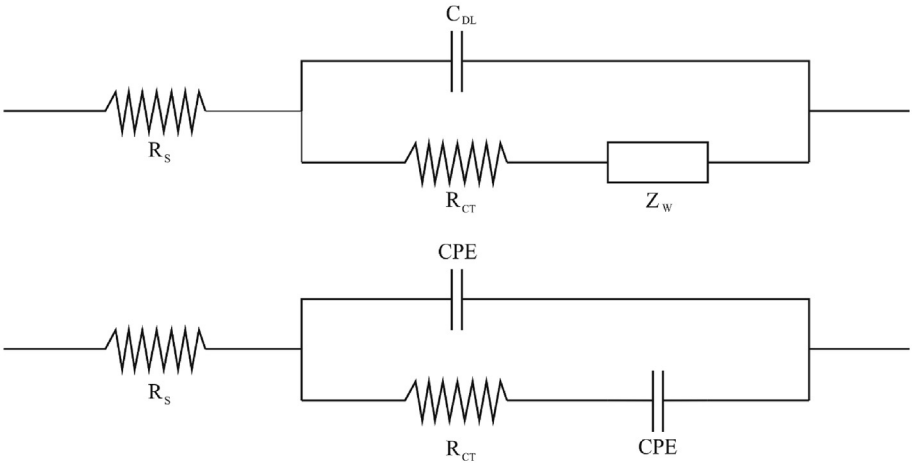

Fig. 2. Equivalent circuit models utilised for estimating EIS parameters. A: Randles circuit; B: modified Randles circuit for diffusionless electrode processes.

observed to increase regularly according to the Randles-Ševćik equation for a reversible reaction:

$$I_P = \pm 0.4463 nFAC\left(\frac{nF\upsilon D}{RT}\right)^{\frac{1}{2}} \quad (11)$$

where I_P is the peak current, and n, F, D, A, C, υ, R and T have been defined previously. The ΔE_P is observed to increase as the scan rate increases, indicating a quasi-reversible system due to the rate of mass transport being approximately equal to the rate of electron transfer. In the case of 100 mV s^{-1}, for example, the ΔE_P for dopamine corresponds to +210 mV, which increases to +350 mV when the applied scan rate is increased to 400 mV s^{-1}. Similarly in the case of hydroquinone, the ΔE_P of +280 mV at 10 mV s^{-1} increases to +580 mV when the applied scan rate is increased to 400 mV s^{-1}. These increases are converted into ψ values, which are plotted against $[\pi DnF\nu/RT]^{-1/2}$, and presented inset in Fig. 3A and B for the respective analytes. The slope is then equal to k^0 as in Equation (1); the values correspond to 3.30×10^{-3} and 5.18×10^{-4} cm s^{-1} for dopamine and hydroquinone, respectively, using an ESPE electrode. The result for dopamine is in excellent agreement with values reported for a glassy carbon electrode [18].

Equation (6) describes the relationship between k^0 and R_{CT}, two quantities which are related to the concentration of the electroactive species. In order to make this equation algebraic and functional as a linear plot, it can be expressed as:

$$R_{CT} = \frac{RT}{n^2F^2Ak^0}.\frac{1}{C}. \quad (12)$$

We now have a simple mathematical expression for R_{CT} in terms of the concentration and, given that the remainder of the equation contains known quantities (with the exception of k^0), this can be used to graphically measure k^0 [11,13]. Fig. 4 depicts EIS profiles using an ESPE electrode for dopamine and hydroquinone, respectively, where the voltammetric half wave potential (at 100 mV s^{-1}) has been selected as the excitation potential in both cases (+0.13 and + 0.1 V for dopamine and hydroquinone, respectively). The R_{CT} is observed to decrease as a function of concentration in both cases, and is observed in the plots of R_{CT} *versus* the reciprocal of the concentration, inset in Fig. 4A and B. The slope is almost perfectly linear in both cases – for dopamine the R^2 value corresponds to 0.9996, and for hydroquinone the R^2 value corresponds to 0.9968. The % Relative Standard Deviation (RSD) remains lower than 5.5% across the linear range of 50–285 nM for dopamine. Likewise, for hydroquinone, the % RSD remains below 8%

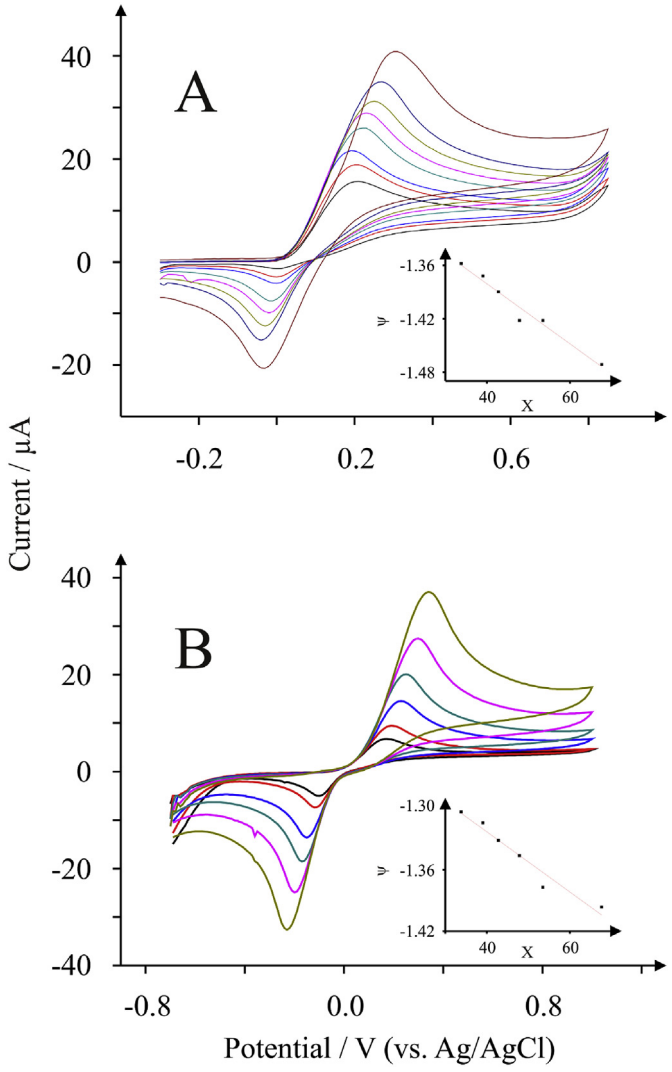

Fig. 3. Scan rate studies for: (A) 0.3 mM dopamine in pH 7.4 PBS with 0.1 M KCl; and (B) 0.6 mM hydroquinone in pH 7.4 PBS. Inset: ψ *versus* X, where $X = [\pi DnF\nu/RT]^{-1/2}$; the slope of which corresponds to k^0.

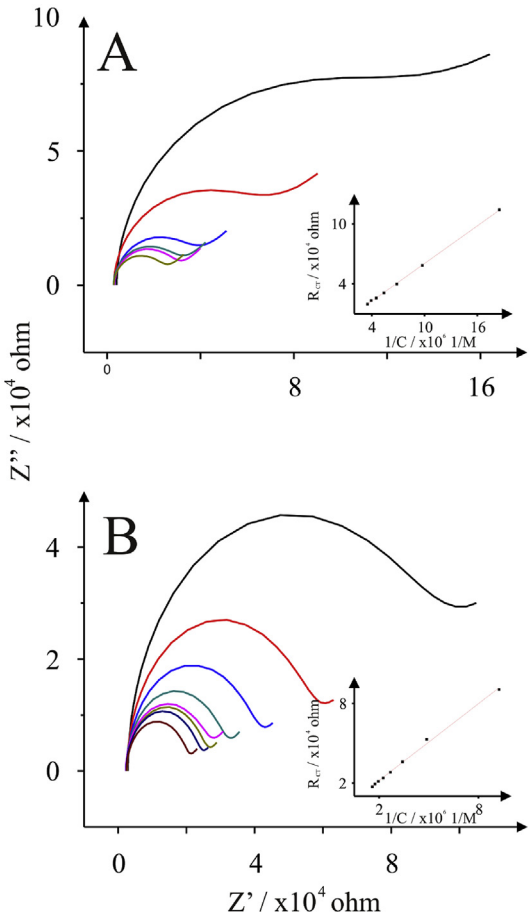

Fig. 4. EIS profiles typical of (A) dopamine and (B) hydroquinone in pH 7.4 PBS and 0.1 M KCl supporting electrolyte. The increasing semicircle diameter is an indication of decreasing concentration. The electrode used in both cases is an ESPE. Inset: R_{CT} *versus* 1/C. Frequency range: 10,000–0.2 Hz; 10 mV ac amplitude; 10 frequencies per decade; DC potential = $E_{1/2}$.

across the linear range of 110–620 nM. For comparative purposes, the concentration versus peak current is investigated *via* CV, using hydroquinone as the model example. In this experiment, the linearity coefficient was slightly less ($R^2 = 0.9929$), and the sensitivity was found to be very high (1.967×10^4 μA mM^{-1}). A decrease in R_{CT} of 9.67 Ω for every unit of 1/C, in the case of EIS is noted.

The rate constants are calculated from the slope of the graph of R_{CT} *versus* the reciprocal of the concentration according to Equation (8), and correspond to 5.98×10^{-4} cm s^{-1} for the case of dopamine and 3.49×10^{-4} cm s^{-1} for the case of hydroquinone. Comparing to CV, where the k^0 values for dopamine and hydroquinone are estimated to be 3.30×10^{-3} and 5.18×10^{-4} cm s^{-1}, respectively, it is seen that in the case of dopamine, CV estimates the rate constant to be one order of magnitude faster, yet in the case of hydroquinone, both methods estimate values of the same order of magnitude. Small k^0 differences can be ascribed to errors such as the % RSD of the SPEs and electrode passivation. In the case of dopamine, however, there is clearly a *major* discrepancy between the heterogeneous electron transfer rates. Consequently, the work now turns towards explaining the different observations by considering the electrochemical mechanisms which are undertaken by both molecules.

It is well known that dopamine undergoes a complex electrochemical mechanism. In aqueous solutions, the likelihood is that an EC-type reaction is taking place, depicted in Scheme 2. There is a two electron, two proton electrochemical oxidation step initially, which is followed by the chemical step, which is a Michael addition of the primary amine group to position 6 on the aromatic ring [19]. This intramolecular reaction, coupled with potential intermolecular polymerisation reactions, is likely to increase the observed impedance *via* electrode passivation; that is, a collection of unreactive adsorbed material upon the electrode surface hindering electrochemical reactions between the diffusion layer and the electrode material. This is but one of countless proposed dopamine reaction pathways [20]; however regardless of the mechanism, there is an agreement that the electrochemical step is followed by a chemical step, making this a complex mechanism. This creates a limitation for EIS because the experiment is conducted over a longer time frame than voltammetry, meaning that passivation is more likely to occur, which in turn may affect the returned k^0 estimation. It is known that dopamine polymerises and adsorbs upon electrode surfaces [21,22] and could be further increasing R_{CT} values in this case. If the EIS profiles in Fig. 4A and B are compared, it is apparent that in the case of dopamine the semicircle is more depressed than the case for hydroquinone, which is a good indication of a system that is deviating from ideal behaviour. This could be due to electrode passivation resulting from polymerisation and could explain the higher impedances observed in the case of dopamine. Hydroquinone on the other hand is a much simpler, two-proton, two-electron reaction (or perhaps two one-proton, one-electron processes combined) mechanism with little polymerisation, intra/intermolecular reactions, or surface reactions

Table 3
Summary of the heterogeneous electron transfer rate constants for hydroquinone, utilising the four SPEs, calculated using EIS and CV. %RSD values are provided ($N = 3$).

Electrode	CV $k^0/10^{-4}$ cm s^{-1} (%RSD[a])	EIS $k^0/10^{-4}$ cm s^{-1} (%RSD)
ESPE	5.18 (0.019)	3.49 (3.95)
BSPE	2.77 (5.66)	3.30 (9.40)
GSPE	0.488 (2.85)	2.49 (8.95)
LRI-SPE	2.71 (2.26)	2.69 (7.76)

[a] Taken from data produced in Reference [14].

[23]. In the case of hydroquinone, the electron transfer rate constants are found to be similar using both methods. However as this is not the case for dopamine, the non-Faradaic processes are looked upon as being responsible for the difference. This work infers that these methods are only applicable for simple electron transfer, as is assumed in the case of hydroquinone.

Considered next are the limitations of this approach. While the plot of R_{CT} versus 1/C is extremely linear, there are large errors in all cases when the concentration approaches sufficiently low (50 μM) or sufficiently high (1 mM) concentrations. As the concentration approaches zero, the EIS profile tends to be more unpredictable, which could be an effect of the high dielectric constant of water. The upper limit is likely due to a high ionic strength causing deviations according to the Debeye-Hückel limiting law. Indeed, if attention is paid to the graphs inset of Fig. 4A and B, it is apparent that the data points are deviating from linearity as the concentration increases. Therefore it is advised that this method can only be operated within a small concentration range. There is an added limitation that this method cannot be utilised in circumstances where the electrochemical mechanism is unknown because the method appears to be limited to simple systems.

It is necessary to explore different carbon substrates in order to understand whether anisotropic effects of the carbon materials affect the observed impedances utilising EIS. Furthermore, it is useful to compare EIS- and CV-determined k^0 values, because theoretically they should be the same. Table 3 summarises the k^0 values determined *via* CV and EIS, and it is immediately apparent that in some cases the k^0 values are measured to be similar, and in others, the k^0 values are found to be significantly different. The case of the ESPE sees a CV-determined k^0 value of 5.18×10^{-4} cm s^{-1} reduce to 3.49×10^{-4} cm s^{-1} when determined by EIS. This decrease is an approximate 33% decrease which is a significant difference, even if the order of magnitude is the same. It is believed that the density of states has little to do with the differences observed between techniques, because the case of the GSPE sees the k^0 values to be the same value for both CV and EIS (2.70×10^{-4} cm s^{-1}). Therefore if the similar density of states exhibited by both electrodes from previous work is ignored [14], there must be another constituent of the inks which is contributing to the changes in observed k^0. The lack of information from the manufacturer reduces our capability to critically analyse the ink further. However, it can be speculated that polymeric binders play a

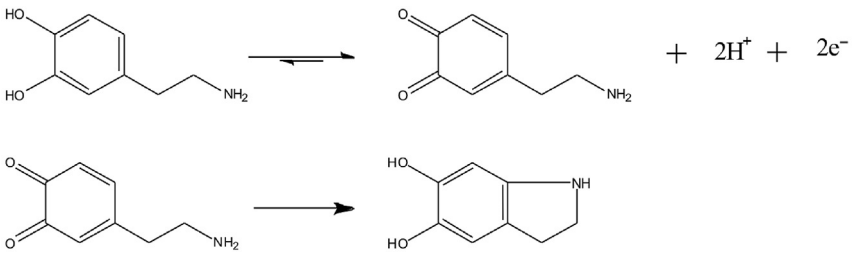

Scheme 2. Electrochemical mechanism associated with dopamine [19].

role in reducing the EIS-determined k^0 values. The BPSE is an ink which contains polymeric binder, as determined in our previous work [14]. In the present work, a large disparity is seen between the CV-determined k^0 (4.88×10^{-5} cm s^{-1}) and the EIS-determined k^0 (2.49×10^{-4} cm s^{-1}) which is an order of magnitude different. In this case, the longer experimental timeframe of EIS appears to aid in the estimation of the k^0 value. The BSPE ink is designed to exhibit slow electron transfer kinetics by "blocking" the carbon active sites by mixing polymers into the matrix. Clearly in this case, the voltammetric currents are being affected dramatically by the binders in the ink. The case of the LRI-SPE sees the k^0 value of 2.77×10^{-4} *via* CV increase to 3.30×10^{-4} *via* EIS, equating to a percentage increase of approximately 20%. To summarise, the magnitude of the CV-determined k^0 decreases in the order ESPE > LRI-SPE > GSPE » BSPE. One would expect ESPE, GPSE, and perhaps even LRI-SPE to exhibit similar voltammetry as was the case with previous work [14]. The slight differences (at least, in the case of ESPE and GSPE) can be ascribed to the slight differences in surface oxygen content, which is well known to affect observed voltammetry [14]. On the other hand, the EIS-determined k^0 values decrease in the order ESPE > GSPE > LRI-SPE » BSPE. For the EIS case, the k^0 is inversely proportional to the R_{CT} as described by Equation (8). Therefore, a higher k^0 alludes to a lower overall impedance. In terms of the ESPE, this would be expected this to exhibit the highest because the Faradaic process is clearly the quickest at this electrode than the other three, according to the voltammetric results. Additionally, BSPE is expected to exhibit the slowest electron transfer because of the high polymer content. From the data presented, ESPE is the best electrode to use for both cases.

Finally the knowledge gained above is used to test electrochemically irreversible analytes as the k^0 values cannot be estimated experimentally using the Nicholson method. We know that Equation (9) can be used in cases where there is simple electron transfer. For the purposes of this section, assume the electron transfer processes to be simple. EIS becomes advantageous over CV for electrochemically irreversible systems because the k^0 value is measured from only one charge transfer reaction instead of two. Fig. 5 displays EIS profiles for ascorbic acid and norepinephrine using an LRI-SPE, accompanied by plots of R_{CT} *versus* the reciprocal of the concentration. In the case of ascorbic acid, the slope corresponds to 0.1657, which when substituted into Equation (8), gives a k^0 value corresponding to 8.04×10^{-5} cm s^{-1}. This value is logical considering the electrochemical irreversibility of ascorbic acid; thus it could be argued that this is a reasonable estimate for the rate of electron transfer because electron transfer is limiting the electrode processes. Similarly, in the case of norepinephrine, the apparent k^0 value is estimated to be 1.29×10^{-4} cm s^{-1}, using the same method. Again, this is a slow electron transfer rate of a similar magnitude to the case of ascorbic acid. One would expect norepinephrine to be slightly quicker due to the smaller potential required for the electrode process to proceed. Scan rate studies were also performed on the two analytes to acquire information for use in Digisim, a program that computes electron transfer rate constants for electrochemically irreversible systems. The obtained data is tabulated in Table 4, which highlights a huge disparity between the experimentally determined and simulated k^0 values for electrochemically irreversible systems. In the case of norepinephrine, Digisim™ estimates the rate constant to be 9.90×10^{-9} cm s^{-1}, which is very slow and, though an electrochemically irreversible system, is low enough to warrant suspicion. The case of ascorbic acid estimates the k^0 to correspond to 6.20×10^{-6} cm s^{-1}, which is more believable for an electrochemically irreversible system, and is one order of magnitude slower than EIS. If the mechanism of norepinephrine, an ECCE mechanism [24], is considered, it is clear that complicated electrode processes are unsuitable for this data

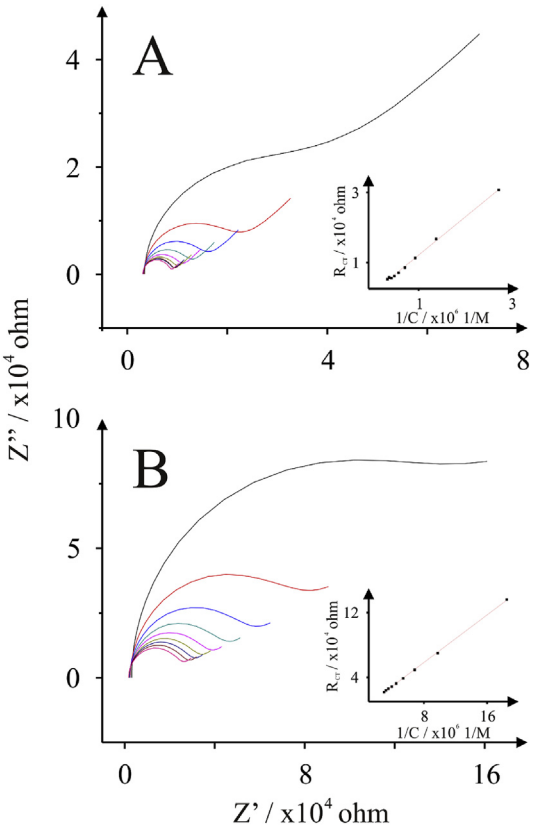

Fig. 5. EIS spectra for (A) ascorbic acid and (B) norepinephrine. Inset: R_{CT} *versus* 1/C. 10,000–0.2 Hz; 10 mV ac amplitude; 10 frequencies per decade; DC potential = $E_{1/2}$.

Table 4
EIS- and Digisim-determined rate constants for ascorbic acid and norepinephrine.

Analyte	EIS-determined k^0/cm s^{-1}	Digisim-determined k^0/cm s^{-1}
Ascorbic acid	8.04×10^{-5}	6.20×10^{-6}
Norepinephrine	1.29×10^{-4}	9.90×10^{-9}

analysis. Ascorbic acid, on the other hand, undergoes a much simpler electron transfer process (two electron, one proton [25]) with no chemical steps involved. Therefore, it appears from this evidence that the Digisim™ estimations are probably valid for simple processes. Similarly with EIS, the predicted k^0 value for norepinephrine may be a more reasonable estimate than Digisim™, the ECCE nature may affect the k^0 value using this method.

Such critical assessment of k^0 between methods is, to the best of the author's knowledge, the first of its kind and has been reported for users of EIS to use and improve their data analysis.

4. Conclusions

The electron transfer rate constants deduced from CV and EIS have been critically analysed and compared. This paper has proved that there is a difference between the k^0 values obtained *via* both methods of approximately one order of magnitude for the case of dopamine, yet in the case of hydroquinone, both methods predict similar rate constants for a range of carbon electrodes. It has been demonstrated that for complex electrochemical systems such as dopamine, the non-Faradaic contributions appear to contribute to the R_{CT} component and the method currently only appears to be valid for simple electron processes. The observations in linking k^0 to

the concentration have been applied to be used for the estimation of the k^0 values for two electrochemically irreversible systems (ascorbic acid and norepinephrine) with some success. Digital simulations have been acquired to compare and contrast EIS-predicted rate constants and there has been a large disparity in the predicted rate constants between the two methods, when the electrochemical oxidation of the analyte is a complicated electrode process. Therefore, EIS and Digisim comparisons should, for the moment, be strictly limited to simple electrode processes.

The procedures utilised within this paper exhibit some unfortunate limitations. Operation below concentrations of 50 μM or in excess of 1 mM is ill-advised, due to deviations in linearity. The method should be limited to simple electron processes. While this work stands as a proof-of-concept approach, it has potential to become a widely utilised method both electroanalytically for users who want to use EIS to deduce concentrations of target species within unknown samples, and qualitatively in cases where electron transfer rate constants are required to study electrode materials for applications such as fuel cell and battery research.

Declaration of interest

The author declares no conflicts of interest with this work.

Acknowledgements

Edward Randviir acknowledges Professor Craig Banks for use of research equipment and Professor Frank Marken for his support in the writing of the manuscript.

References

[1] E.P. Randviir, D.A.C. Brownson, C.E. Banks, Mater. Today, 17, 426-432.
[2] R.A. Marcus, J. Chem. Phys. 24 (1956) 966–978.
[3] R.A. Marcus, J. Chem. Phys. 26 (1957) 867–871.
[4] R.A. Marcus, Rev. Mod. Phys. 65 (1993) 599–610.
[5] J.E.B. Randles, Discuss. Faraday Soc. 1 (1947) 11–19.
[6] R.S. Nicholson, I. Shain, Anal. Chem. 36 (1964) 706–723.
[7] R.S. Nicholson, Anal. Chem. 38 (1966), 1406-1406.
[8] R.S. Nicholson, Anal. Chem. 37 (1965) 1351–1355.
[9] I. Lavagnini, R. Antiochia, F. Magno, Electroanalysis 16 (2004) 505–506.
[10] A.J. Bard, L.R. Faulkner, Electrochemical Methods: Fundamentals and Applications, Wiley, 2000.
[11] J.H. Sluyters, J.J.C. Oomen, Recl. Trav. Chim. Pays-Bas 79 (1960) 1101–1110.
[12] E.P. Randviir, C.E. Banks, Anal. Methods 5 (2013) 1098–1115.
[13] J.H. Sluyters, Recl. Trav. Chim. Pays-Bas 79 (1960) 1092–1100.
[14] E.P. Randviir, D.A.C. Brownson, J.P. Metters, R.O. Kadara, C.E. Banks, Phys. Chem. Chem. Phys. 16 (2014) 4598–4611.
[15] N.A. Choudry, D.K. Kampouris, R.O. Kadara, C.E. Banks, Electrochem. Commun. 12 (2010) 6–9.
[16] J.P. Smith, J.P. Metters, D.K. Kampouris, C. Lledo-Fernandez, O.B. Sutcliffe, C.E. Banks, Analyst 138 (2013) 6185–6191.
[17] L.R. Cumba, C.W. Foster, D.A.C. Brownson, J.P. Smith, J. Iniesta, B. Thakur, D.R. do Carmo, C.E. Banks, Analyst 141 (2016) 2791–2799.
[18] A. Curulli, F. Valentini, S. Orlanducci, M.L. Terranova, Indian J. Chem. 44A (2005) 956–967.
[19] S. Shahrokhian, S. Bozorgzadeh, Electrochim. Acta 51 (2006) 4271–4276.
[20] S. Corona-Avendaño, G. Alarcón-Angeles, M.T. Ramírez-Silva, G. Rosquete-Pina, M. Romero-Romo, M. Palomar-Pardavé, J. Electroanal. Chem. 609 (2007) 17–26.
[21] A. Hermans, Fabrication and Applications of Dopamine-sensitive Electrodes, ProQuest, 2007.
[22] E. Ekinci, G. Erdogdu, A.E. Karagözler, Polym. Bull. 44 (2000) 547–553.
[23] T.A. Enache, A.M. Oliveira-Brett, J. Electroanal. Chem. 655 (2011) 9–16.
[24] C. Bian, Q. Zeng, H. Xiong, X. Zhang, S. Wang, Bioelectrochemistry 79 (2010) 1–5.
[25] M.R. Deakin, P.M. Kovach, K.J. Stutts, R.M. Wightman, Anal. Chem. 58 (1986) 1474–1480.
[26] N. Siraj, G. Grampp, S. Landgraf, K. Punyain, Z. Phys. Chem. Int. J. Res. Phys. Chem. Chem. Phys. (2013) 105.
[27] R. Feeney, S.P. Kounaves, Electrochem. Commun. 1 (1999) 453–458.
[28] M.E. Ortiz, L.J. Núñez-Vergara, J.A. Squella, J. Electroanal. Chem. 549 (2003) 157–160.
[29] C.W. Foster, J.P. Metters, D.K. Kampouris, C.E. Banks, Electroanalysis 26 (2014) 262–274.
[30] D.A.C. Brownson, S.A. Varey, F. Hussain, S.J. Haigh, C.E. Banks, Nanoscale 6 (2014) 1607–1621.
[31] N.K. Bhatti, M.S. Subhani, A.Y. Khan, R. Qureshi, A. Rahman, Turk. J. Chem. 29 (2005) 659–668.
[32] V. Ganesh, S.K. Pal, S. Kumar, V. Lakshminarayanan, J. Colloid Interface Sci. 296 (2006) 195–203.
[33] F. Sundfors, J. Bobacka, A. Ivaska, A. Lewenstam, Electrochim. Acta 47 (2002) 2245–2251.
[34] C. Saby, B. Ortiz, G.Y. Champagne, D. Bélanger, Langmuir 13 (1997) 6805–6813.
[35] A.M. Oliveira-Brett, L.A.d. Silva, C.M.A. Brett, Langmuir 18 (2002) 2326–2330.
[36] F. Cruz Moraes, M.F. Cabral, S.A.S. Machado, L.H. Mascaro, Electroanalysis 20 (2008) 851–857.